The Journal of Chemical Physics

Application of XDM to ionic solids: The importance of dispersion for bulk moduli and crystal geometries

Cite as: J. Chem. Phys. **153**, 054121 (2020); https://doi.org/10.1063/5.0015133
Submitted: 25 May 2020 . Accepted: 19 July 2020 . Published Online: 06 August 2020

A. Otero-de-la-Roza, and Erin R. Johnson

The Journal of Chemical Physics ARTICLE scitation.org/journal/jcp

Application of XDM to ionic solids: The importance of dispersion for bulk moduli and crystal geometries

Cite as: J. Chem. Phys. 153, 054121 (2020); doi: 10.1063/5.0015133
Submitted: 25 May 2020 • Accepted: 19 July 2020 •
Published Online: 6 August 2020

A. Otero-de-la-Roza[1,a] and Erin R. Johnson[2,b]

AFFILIATIONS

[1] Departamento de Química Física y Analítica and MALTA Consolider Team, Facultad de Química, Universidad de Oviedo, 33006 Oviedo, Spain

[2] Department of Chemistry, Dalhousie University, 6274 Coburg Rd., Halifax, Nova Scotia B3H 4R2, Canada

[a] **Author to whom correspondence should be addressed:** aoterodelaroza@gmail.com
[b] **Electronic mail:** erin.johnson@dal.ca

ABSTRACT

Dispersion corrections are essential in the description of intermolecular interactions; however, dispersion-corrected functionals must also be transferrable to hard solids. The exchange-hole dipole moment (XDM) model has demonstrated excellent performance for non-covalent interactions. In this article, we examine its ability to describe the relative stability, geometry, and compressibility of simple ionic solids. For the specific cases of the cesium halides, XDM-corrected functionals correctly predict the energy ranking of the B1 and B2 forms, and a dispersion contribution is required to obtain this result. Furthermore, for the lattice constants of the 20 alkali halides, the performance of XDM-corrected functionals is excellent, provided that the base functional's exchange enhancement factor properly captures non-bonded repulsion. The mean absolute errors in lattice constants obtained with B86bPBE-XDM and B86bPBE-25X-XDM are 0.060 Å and 0.039 Å, respectively, suggesting that delocalization error also plays a minor role in these systems. Finally, we considered the calculation of bulk moduli for alkali halides and alkaline-earth oxides. Previous claims in the literature that simple generalized gradient approximations, such as PBE, can reliably predict experimental bulk moduli have benefited from large error cancellations between neglecting both dispersion and vibrational effects. If vibrational effects are taken into account, dispersion-corrected functionals are quite accurate (4 GPa–5 GPa average error), again, if non-bonded repulsion is correctly represented. Careful comparisons of the calculated bulk moduli with experimental data are needed to avoid systematic biases and misleading conclusions.

I. INTRODUCTION

London dispersion plays a critical role in determining the structure and energetics of molecular aggregates, molecular crystals, and layered materials.[1,2] However, it has been shown that dispersion can also affect the description of solids where van der Waals interactions are not usually thought to be important. For instance, although electrostatics is the main contribution to binding in ionic solids, inclusion of dispersion has been shown to improve the quality of the computed lattice constants and atomization energies significantly.[3,4] As another example, density-functional calculations without dispersion incorrectly predict the rocksalt (B1) structure to be lower in energy than the cesium-chloride (B2) form of CsCl, CsBr, and CsI under ambient conditions.[5,6]

Over the last 15 years, a number of dispersion corrections and dispersion-including functionals have been developed in the context of density-functional theory (DFT).[1,2,7,8] These include asymptotic dispersion corrections,[9–20] non-local density functionals,[21–27] dispersion-correcting potentials,[28–33] and parameterized exchange–correlation functionals,[34–38] among others.[39–43] Beyond-DFT methods, such as the random-phase approximation (RPA), also capture dispersion interactions.[5,44] The class of asymptotic dispersion

corrections includes several generations of Grimme's models (D2,[9] D3,[10,11] and D4[12,13]), the Tkatchenko–Scheffler (TS)[14] and subsequent many-body dispersion (MBD)[15] methods, and the exchange-hole dipole moment (XDM) dispersion correction.[16,45] Additional improvements on the MBD model have been proposed to account for polarizability variations due to fractional atomic charges, as in MBD-FI[46] and uMBD.[47]

In an asymptotic pairwise dispersion correction, the dispersion energy is written as a sum over atomic pairs using a damped asymptotic energy expression, as motivated by second-order perturbation theory.[48,49] The leading-order dispersion term in these corrections is

$$E_{\mathrm{disp}}^{(6)} = -\sum_{i<j} \frac{C_{6,ij} f_{6,ij}(R_{ij})}{R_{ij}^6}, \tag{1}$$

where the sum runs over all atom pairs, the $C_{6,ij}$'s are the dispersion coefficients, and $f_{6,ij}(R_{ij})$ is a damping function introduced to avoid divergence at short internuclear separations, R_{ij}. The development and benchmarking of asymptotic pairwise dispersion corrections are important because they attain good accuracy and can be applied in combination with common, thoroughly tested density-functional approximations. Furthermore, these methods are computationally very simple with a much lower cost than non-local dispersion functionals or the more complicated MBD-based methods, extending their range of applicability to larger chemical systems.

The various asymptotic dispersion corrections primarily differ in how the dispersion coefficients are computed, although there are also differences in whether higher-order dispersion-energy terms (i.e., C_8 or C_{10}) are included, and in the choice of damping function. However, all of these dispersion corrections are in some way dependent on reference data for neutral atoms or compounds, and only the D4 method[12] (very recently implemented for periodic solids[13]) was specifically designed with ionic systems in mind. It is therefore uncertain how such asymptotic dispersion models perform for ionic solids. Previous assessments for alkali halides demonstrated a very poor performance of the TS method and convergence failures of MBD.[3] While addition of the D2 or D3 corrections results in significant improvements over uncorrected base functionals,[5,6] they are still considerably less accurate than dispersion corrections tailor-made for ionic crystals.[3]

All dispersion corrections have been designed with the purpose of accurately describing non-covalent interactions, either in molecules or in solids. However, if these methods are to be applied to complex systems that involve not only van der Waals interactions but also other bonding types (covalent, ionic, and metallic), then it is crucial that those other interactions are correctly represented as well. In addition, given that systems where non-covalent interactions are important are typically large, it would be preferable to have a dispersion-corrected functional that is as simple as possible. This would ideally be an asymptotic pairwise dispersion correction paired with a GGA (generalized gradient approximation) functional due to favorable scaling and the simplicity of their computational implementation. In this work, we focus on the XDM dispersion method, which has been shown to provide simultaneously excellent performance for gas-phase molecules,[50,51] molecular crystals,[52–56] surface adsorption,[57–60] and layered materials[61,62] in combination with GGA base functionals, without any modification or reparameterization. Indeed, XDM is at present the only pairwise asymptotic dispersion model that is able to provide an accurate description of both the cell parameters and exfoliation energies of layered transition-metal dichalcogenides.[62,63] (Some variants of non-local van der Waals functionals and MBD-FI[46] also describe these systems accurately.[62])

In order to complete the exploration of XDM-corrected functionals, we address herein their ability to correctly predict the stable polymorphs of the cesium halides, as well as the lattice parameters and bulk moduli of 20 alkali halides and 4 alkaline-earth oxides. The accurate calculation of relative stabilities, geometries, and bulk moduli has been shown to be essential for the prediction of many other thermodynamic properties in simple solids.[64,65] These ionic systems have been studied in the literature using dispersion methods other than XDM,[3–6] and we also address some of the difficulties with these previous works regarding the comparison with experimental data for bulk moduli.

II. COMPUTATIONAL METHODS

Calculations were performed for the alkali halides composed of all combinations of the Li, Na, K, Rb, and Cs cations and the F, Cl, Br, and I anions, as well as MgO, CaO, SrO, and BaO. At ambient pressure and temperature, all of these compounds present the rocksalt (B1) structure, as shown in Fig. 1, except for CsCl, CsBr, and CsI, which have the CsCl (B2) structure. For each compound, energy vs volume curves were constructed by varying the lattice constants from 70% to 120% of their equilibrium values, and phonon frequencies were computed at each geometry. As all atoms occupy symmetry-fixed sites, all calculations were single-point energy evaluations and no further relaxation was required.

Our calculations used the exchange-hole dipole moment (XDM) dispersion method. XDM is a pairwise asymptotic dispersion correction, in which the dispersion energy is

$$E_{\mathrm{disp}} = -\sum_{n=6,8,10} \sum_{i<j} \frac{C_{n,ij} f_n(R_{ij})}{R_{ij}^n}, \tag{2}$$

where $C_{n,ij}$ are the pairwise dispersion coefficients, f_n is the damping function for the order-n dispersion term, and R_{ij} is the distance

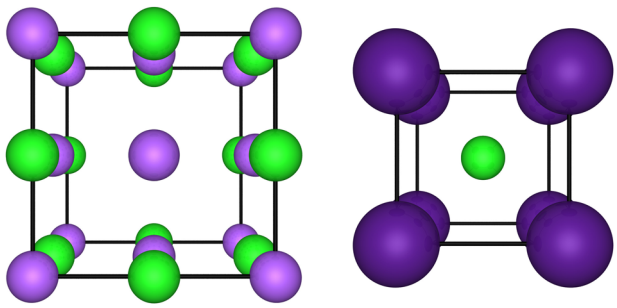

FIG. 1. Conventional unit cells of sodium chloride [B1 (a)] and cesium chloride [B2 (b)]. The alkali cations are shown in purple and the halide anions in green.

between atoms i and j. The XDM dispersion energy contains only two adjustable parameters (a_1 and a_2) used in all Becke–Johnson damping functions,[66]

$$f_n(R) = \frac{R^n}{R^n + (a_1 R_c + a_2)^n}, \tag{3}$$

where R_c is the critical radius, computed from ratios of the dispersion coefficients of the interacting atoms. The purpose of the damping function parameters is to match the XDM energy with the long-range exchange–correlation from the base functional, and they are determined by fitting to a benchmark set of molecular dimer binding energies.[50,61] After this initial fitting, the a_1 and a_2 values are never reparameterized for specific systems. In XDM, the dispersion coefficients ($C_{n,ij}$) are computed from the self-consistent Kohn–Sham states based on the assumption that dispersion originates from the interaction between dipoles formed by the electrons plus their exchange(–correlation) holes. In this way, XDM captures the physically correct evolution of the C_n coefficients with the atomic chemical environment[62] while, at the same time, retaining the simplicity and cost-efficiency of an asymptotic dispersion correction. The three-body and higher-order coefficients can be calculated as well,[67,68] but are not included in the standard XDM implementation. A more in-depth description of XDM has been given elsewhere.[16,45,68,69]

In this work, the XDM dispersion correction is paired with either the PBE[70] or B86bPBE[70,71] GGA functionals. PBE is the more popular functional in the materials community, but B86bPBE is the recommended functional to be paired with XDM for solid-state calculations due to its desirable behavior in the limit of large reduced density gradients.[16,72–75] Additional calculations were also performed for a hybrid functional[76] based on B86bPBE with 25% exact exchange,[77] termed B86bPBE-25X.[78]

All calculations used version 6.1 of the Quantum ESPRESSO program,[79] with an 8 × 8 × 8 uniform $\boldsymbol{k}$-point mesh and plane wave cutoffs of 80 and 800 Ry for the kinetic energy and electron density, respectively. We employed the projector augmented wave (PAW) method.[80] Phonon frequencies were calculated at each volume using density-functional perturbation theory (DFPT)[81] with a 4 × 4 × 4 $\boldsymbol{q}$-point mesh. The XDM damping function parameters were set to their established literature values of 0.3275 Å and 2.7673 Å for PBE,[16] 0.6512 and 1.4633 Å for B86bPBE,[16] and 0.6754 Å and 1.4651 Å for B86bPBE-25X.[78] We use the canonical version of XDM with pairwise C_6, C_8, and C_{10} terms, but no atomic three-body dispersion, which has been shown to give a negligible contribution in alkali halides,[3] in general.[68] We note that the XDM pairwise dispersion coefficients do include electronic many-body effects.[68]

The $E(V)$ curves, combined with the phonon frequencies at each volume, were used to calculate the thermodynamic properties of each crystal using the Gibbs2 program.[82,83] At zero pressure and temperature, T, the Gibbs energy can be computed from the DFT electronic energy (E_{el}) and the vibrational Helmholtz free energy (F_{vib}),

$$G(V,T) = F(V,T) = E_{el}(V) + F_{vib}(V,T). \tag{4}$$

Here, F_{vib} can be calculated as

$$F_{vib}(V,T) = \int \left[\frac{\omega}{2} + k_B T \ln\left(1 - e^{-\frac{\omega}{k_B T}}\right)\right] g(\omega)\, d\omega, \tag{5}$$

where ω is the vibration frequency, $g(\omega)$ is the phonon density of states obtained from DFPT, and k_B is Boltzmann's constant. In the quasi-harmonic approximation (QHA), we introduce anharmonicity by making $g(\omega)$ dependent on the volume. At a given temperature and zero pressure, the equilibrium volume, $V(T)$, the lattice parameters, and bulk modulus are found by minimizing $G(V, T)$.

A computationally simpler alternative to the full QHA, which requires the DFPT phonon density of states at each volume, is the Debye model.[84–86] In this model, the phonon density of states is taken to be a parabola whose curvature is determined by the Debye frequency, ω_D,

$$g_{\text{Debye}}(\omega) = \begin{cases} \frac{9n\omega^2}{\omega_D^3}, & \omega < \omega_D \\ 0, & \omega \geq \omega_D, \end{cases} \tag{6}$$

where n is the number of atoms in the unit cell and $\omega_D = k_B \Theta_D$. Θ_D is the Debye temperature, which can be computed from the static lattice parameter (a_0) and bulk modulus [$B_0 = V(\partial^2 E_{el}/\partial V^2)$] as

$$\Theta_D = \frac{f(\sigma)}{k_B}\left(6\pi^2 n\right)^{1/3}\sqrt{\frac{a_0 B_0}{M}}, \tag{7}$$

where M is the molecular mass and $f(\sigma)$ is a function of the Poisson ratio, usually taken to be $\sigma = \frac{1}{4}$ for simplicity.[83,86] The advantage of the Debye model in this formulation is that it only requires the $E(V)$ curve as input data, greatly simplifying the calculation. The Debye model has been shown to be appropriate in the description of alkali halides.[87]

Two important properties that determine the compressibility of a solid are the isothermal (B_T) and adiabatic (B_S) bulk moduli. The isothermal bulk modulus is

$$B_T = V\left(\frac{\partial^2 F}{\partial V^2}\right)_T, \tag{8}$$

and the adiabatic bulk modulus is

$$B_S = V\left(\frac{\partial^2 U}{\partial V^2}\right)_S = B_T(1 + \alpha\gamma T), \tag{9}$$

where U is the internal energy, α is the coefficient of thermal expansion, and γ is the Grüneisen parameter.[83]

III. RESULTS

A. Cesium-halide polymorphism

Following previous studies in the literature,[5,6] we first consider the relative stabilities of the B1 and B2 cesium-halide polymorphs predicted by XDM-corrected functionals. Experimentally, CsF adopts the B1 structure at room temperature and pressure, while the remaining cesium halides (CsCl, CsBr, and CsI) all favor the B2 phase. The calculated energy differences between the B1 and B2 phases of the cesium halides are shown in Fig. 2 using the B86bPBE and B86bPBE-25X functionals, with (ΔE_{XDM}) and without (ΔE_{base})

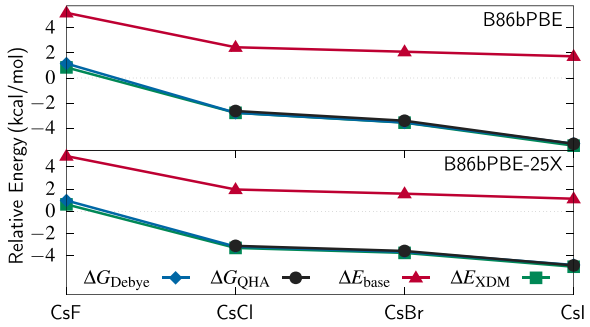

FIG. 2. Relative static energies (ΔE) and Gibbs free energies (ΔG) of the B1 and B2 phases of the Cs halides. A negative value indicates that the B2 phase is more stable. The curves are the Debye (ΔG_{Debye}) and full QHA (ΔG_{QHA}) Gibbs free-energy differences and the static energy differences with (ΔE_{XDM}) and without (ΔE_{base}) dispersion.

the XDM dispersion correction. Without dispersion, both base functionals incorrectly predict the B1 form to be stable for all four cesium halides. The addition of the XDM dispersion term recovers agreement with experiment, and the inclusion of exact exchange has only a minimal effect on the results. This is in agreement with similar observations in the literature using other dispersion corrections.[5,6] The addition of the D2 dispersion correction to PBE, the addition of the D3 or rVV10[88] dispersion corrections to the SCAN functional,[89] and the use of several methods based on the random-phase approximation, were also found to favor the B2 phase for CsCl, CsBr, and CsI.[5] Thus, while inclusion of dispersion is clearly needed to identify the correct stable polymorph in cesium halides, the energy ranking is largely insensitive to the choice of dispersion correction.

The calculated energy differences per formula unit are 0.84 (CsF), −2.77 (CsCl), −3.56 (CsBr), and −5.39 kcal/mol (CsI) using B86bPBE-XDM, and 0.63 (CsF), −3.30 (CsCl), −3.74 (CsBr), and −4.99 (CsI) using B86bPBE-25X-XDM. These values are comparable to those reported using other dispersion-corrected functionals for CsCl:[6] −4.46 (PBEsol-D2), −5.19 (HSE06-D2), and −5.33 kcal/mol (PBE0-D2), although they significantly favor the B2 phase compared to RPA[5] data: 3.26 (CsF), −0.28 (CsCl), −0.55 (CsBr), and −0.57 kcal/mol (CsI). Given that this over-stabilization of the B2 phase is common to most functionals and dispersion corrections (see also Ref. 5), it is possible that its origin lies in some underlying deficiency of the density-functional approximations for ionic interactions[90] or with the RPA itself.[44]

Figure 2 also shows the relative free energies of the B1 and B2 phases obtained with B86bPBE-XDM or B86bPBE-25X-XDM at room temperature from either the Debye model (ΔG_{Debye}) or full QHA (ΔG_{QHA}). For CsCl, CsBr, and CsI, the vibrational contribution to relative phase stability is negligible, and $\Delta E \approx \Delta G$ in all cases. We note that QHA calculations could not be performed for the B2 phase of CsF, as this phase becomes dynamically unstable at the room temperature equilibrium volume, a problem, which cannot happen with the simpler Debye model. For the other three Cs halides, results with the Debye model are in excellent agreement with those from full QHA. All results shown for CsCl, CsBr, and CsI will correspond to the B2 phase in the rest of this article.

B. Static lattice constants

Tao *et al.* recently benchmarked several dispersion-corrected DFT methods for the lattice constants of the alkali halides, as well as bulk metals.[3] Their reference data were obtained by back-correcting experimental lattice constants to eliminate vibrational effects, allowing a direct comparison with the static results from DFT optimizations. Table I displays the equilibrium alkali-halide lattice constants obtained using the selected functionals, with the results from Tao *et al.* provided for comparison.

Table I shows the results for three density functionals without dispersion corrections: the LDA (local density approximation) and two GGA functionals, PBE and B86bPBE. The LDA systematically underestimates lattice constants, while they are consistently overestimated with both GGAs. The general trend in the predicted lattice constants of LDA < PBE < B86bPBE follows the known behavior of the exchange enhancement factors of these functionals. The B86bPBE enhancement factor has the highest limit for large density gradients and provides the best agreement with exact exchange.[72–74] Indeed, PBEsol,[91] which has an enhancement factor intermediate between the LDA and PBE, provides the improved lattice constants,[92,93] but, as we show below, this is likely the result of error cancellation between an overbinding exchange functional and the neglect of dispersion effects.

Table I also shows that adding a dispersion correction to either GGA results in a contraction of the unit cell and a reduction in the lattice constant, often leading to improved agreement with experiment. However, the quality of the computed lattice constants is highly dependent on the choice of dispersion correction. These differences can be attributed to the assumptions made in the computation of the leading-order C_6 dispersion coefficients and to the choice of damping function.

As noted by Tao *et al.*,[3] the TS method gives very poor results, overestimating the effect of dispersion and giving errors 3–4 times higher than obtained with the LDA. This could be because the TS dispersion coefficients are computed from neutral free-atom reference values, which are then scaled by a ratio of atom-in-solid to free-atom volumes. The Hirshfeld volumes used in the scaling have only a weak dependence on chemical environment and charge state, resulting in little change from the atomic reference values.[57,94] Improved values may be obtained if the TS method is modified to use iterative Hirshfeld partitioning.[95] The TS method has also been shown to display poor performance for alkali and alkaline-earth metals.[96]

In the D3 method, the dispersion coefficients are obtained from interpolation of values for neutral hydrides, based on the coordination number.[10] In contrast to TS, addition of the D3 dispersion correction to PBE causes only a slight contraction of the lattice constants and still results in systematic overestimation. This error may be due to the zero-damping function used in D3.[10] This damping function may reduce the dispersion energy excessively at the relatively short internuclear separations seen in ionic solids.[11]

TABLE I. Lattice constants (a_0 in Å) for 20 alkali halides computed with the selected density functionals, compared to experimental data, back-corrected to eliminate vibrational effects.[3] The B86bPBE, PBE-XDM, B86bPBE-XDM, and B86bPBE-25X-XDM results are original to this work. Literature data obtained with other functionals are also shown. ME: mean error and MAE: mean absolute error.

	No dispersion			Literature dispersion methods			XDM-corrected methods			
Name	LDA[3]	PBE[3]	B86bPBE	PBE-vdW[3]	PBE-TS[3]	PBE-D3[3]	PBE	B86bPBE	B86bPBE-25X	Expt.[3]
LiF	3.911	4.067	4.075	4.002	3.656	4.001	3.961	4.004	3.960	3.948
LiCl	4.966	5.151	5.167	5.086	4.949	5.085	5.062	5.084	5.077	5.045
LiBr	5.311	5.511	5.534	5.440	5.531	5.436	5.419	5.451	5.459	5.403
LiI	5.807	6.020	6.044	5.942	5.894	5.934	5.892	5.956	5.987	5.883
NaF	4.505	4.699	4.710	4.653	4.866	4.638	4.588	4.570	4.527	4.556
NaCl	5.466	5.697	5.708	5.631	5.377	5.655	5.526	5.522	5.532	5.547
NaBr	5.786	6.036	6.051	5.962	5.586	5.960	5.838	5.841	5.869	5.884
NaI	6.262	6.530	6.551	6.441	6.001	6.410	6.289	6.305	6.351	6.368
KF	5.161	5.419	5.434	5.231	5.151	5.383	5.138	5.215	5.199	5.267
KCl	6.077	6.382	6.400	6.103	5.548	6.383	5.986	6.142	6.167	6.205
KBr	6.372	6.706	6.727	6.421	5.757	6.689	6.257	6.433	6.478	6.503
KI	6.818	7.183	7.196	6.929	6.239	7.094	6.666	6.849	6.912	6.961
RbF	5.462	5.738	5.755	5.558	5.272	5.700	5.408	5.522	5.518	5.559
RbCl	6.378	6.699	6.712	6.436	5.718	6.723	6.221	6.411	6.452	6.498
RbBr	6.667	7.016	7.041	6.716	5.997	7.038	6.489	6.693	6.750	6.803
RbI	7.104	7.486	7.501	7.156	6.646	7.443	6.898	7.100	7.174	7.241
CsF	5.807	6.111	6.149	5.920	5.465	6.075	5.731	5.898	5.900	5.984
CsCl	3.968	4.202	4.226	4.014	3.869	4.198	3.934	4.027	4.041	4.057
CsBr	4.139	4.389	4.413	4.201	3.956	4.388	4.104	4.208	4.228	4.224
CsI	4.402	4.667	4.689	4.466	4.137	4.666	4.340	4.446	4.500	4.491
ME	−0.103	0.164	0.183	−0.006	−0.341	0.124	−0.134	−0.038	−0.017	
MAE	0.103	0.164	0.183	0.058	0.386	0.124	0.143	0.060	0.039	

Table I also shows the performance of several XDM-corrected methods. PBE-XDM gives relatively poor performance, with errors comparable in magnitude to PBE-D3, but opposite in sign. This may be attributed to the balance between the XDM dispersion energy and the PBE base functional. PBE tends to underestimate non-bonded repulsion due to its exchange enhancement factor.[16,72–75] As a result, PBE-XDM typically over-estimates the strength of more polar interactions, such as H-bonding, while underestimating purely dispersive interactions.[50] It therefore follows that PBE-XDM would provide excessive binding in ionic crystals. Conversely, B86bPBE, which is typically the functional of choice to pair with XDM,[16,52,61] gives a more accurate treatment of non-bonded repulsion, providing stiffer potentials than PBE, closer to exact exchange.[72–74] As shown in Table I, B86bPBE-XDM provides lattice constants in good agreement with experiment, with a mean absolute error (MAE) similar to the PBE-vdW method developed specifically for simple bulk solids.[3] We also note that, of the methods considered here, only XDM and the vdW method of Tao *et al.* involve non-empirical dispersion coefficients, which likely explains their improved accuracy for ionic systems by being the only methods that capture electronic many-body effects correctly.[68]

Despite the good performance of B86bPBE-XDM in Table I, the lattice constants remain systematically underestimated with respect to experiment. A possible explanation for this may be delocalization error from the underlying GGA functional,[97–100] which is expected to result in overbinding of ionic materials, and could potentially be reduced with hybrid functionals. This prompted us to consider the performance of the B86bPBE-25X hybrid, paired with XDM. The results in Table I show that B86bPBE-25X-XDM further reduces the errors, and the MAE of 0.039 Å is the lowest obtained with any of the methods considered.

The average errors in the calculation of static equilibrium volumes of alkali halides using B86bPBE-XDM and B86bPBE-25X-XDM are 3.0% and 2.0%, respectively. If only cesium halides are considered, these figures decrease to 2.6% and 1.6%. For comparison, Nepal *et al.* reported the average errors of 2.4% and 1.8% using the random phase approximation (RPA) and beyond-RPA methods for the cesium halides, respectively.[5] The performance of B86bPBE-XDM and B86bPBE-25X-XDM is also comparable to the best-performing non-local functionals reported by Klimeš *et al.*[4]

C. Room-temperature lattice constants

The static lattice constants proposed by Tao *et al.*[3] rely on a back-correction to compare experimental data to static results. However, the vibrational free energy also changes according to the functional, so it is interesting to consider whether lattice constants at a finite temperature predicted with the Debye and full QHA models are equally accurate. In particular, the

B86bPBE-XDM and B86bPBE-25X-XDM functionals have been shown to predict accurate static lattice constants, so we now consider their performance in the calculation of room-temperature lattice constants.

Table II shows our results for the room-temperature (298 K) lattice constants, accounting for thermal expansion via either the Debye or full QHA models. The four alkaline-earth oxides (MgO, CaO, SrO, and BaO) are added to our dataset, as they share the same rocksalt structure with the majority of the alkali halides. Since phonon frequencies cannot be calculated with hybrid functionals in Quantum ESPRESSO, the B86bPBE-XDM phonon densities of states were used in combination with the B86bPBE-25X-XDM electronic energies in the full QHA case.

Before proceeding to the results, we note that the full QHA does not give reliable results for LiCl, LiBr, and LiI. In LiCl, the room-temperature volume was grossly overestimated, whereas in LiBr and LiI, the B1 phases were found to have phonon instabilities at the room-temperature volumes. In all three cases, the root of the problem is the breakdown of the quasiharmonic approximation in the particular case of full QHA beyond ~150 K–200 K. The thermal expansivity, α, is known experimentally to be linear with temperature at high temperature. Wentzcovitch *et al.* proposed the inflection point in the calculated thermal expansivity vs temperature curve as the temperature threshold above which the quasiharmonic approximation is not valid.[101] Figure 3 shows the $\alpha(T)$ curves obtained using B86bPBE-XDM and the full QHA or Debye models. The threshold temperature in full QHA is reached at 200 K, and consequently, the equilibrium volume at higher temperatures is overestimated. The same problem is not present when the Debye model is used.

TABLE II. Computed lattice constants (in Å) obtained with the B86bPBE-XDM and B86bPBE-25X-XDM methods using thermal corrections obtained with either the Debye model (a_{Debye}) or the full quasi-harmonic approximation (a_{QHA}). Experimental data at 298 K[102,103] are included for comparison. ME: mean error and MAE: mean absolute error.

	B86bPBE-XDM		B86bPBE-25X-XDM		Experiment
Name	a_{Debye}	a_{QHA}	a_{Debye}	a_{QHA}	a_{expt}
LiF	4.071	4.060	4.025	4.010	4.017
LiCl	5.168	...	5.158	...	5.130
LiBr	5.537	...	5.543	...	5.501
LiI	6.041	...	6.070	...	6.000
NaF	4.639	4.616	4.594	4.571	4.620
NaCl	5.600	5.576	5.611	5.586	5.641
NaBr	5.926	5.900	5.953	5.929	5.973
NaI	6.402	6.370	6.445	6.418	6.473
KF	5.292	5.260	5.275	5.242	5.347
KCl	6.220	6.192	6.250	6.219	6.293
KBr	6.516	6.487	6.564	6.535	6.600
KI	6.943	6.902	7.008	6.969	7.066
RbF	5.592	5.565	5.589	5.560	5.640
RbCl	6.489	6.454	6.534	6.498	6.581
RbBr	6.777	6.737	6.841	6.797	6.854
RbI	7.198	7.141	7.272	7.220	7.342
CsF	5.961	5.941	5.966	5.944	6.008
CsCl	4.071	4.071	4.093	4.085	4.123
CsBr	4.252	4.252	4.284	4.273	4.286
CsI	4.511	4.511	4.573	4.546	4.567
MgO	4.266	4.259	4.223	4.216	4.211
CaO	4.818	4.810	4.805	4.796	4.810
SrO	5.188	5.182	5.174	5.167	5.160
BaO	5.585	5.585	5.577	5.576	5.523
ME	−0.029	−0.060	−0.014	−0.042	
MAE	0.058	0.077	0.033	0.053	

Table II shows that, in agreement with the static results from Table I, both B86bPBE-XDM and B86bPBE-25X-XDM provide good agreement with the experimental geometries at room temperature. For B86bPBE-XDM, the MAEs are 0.058 Å and 0.077 Å with the Debye and full QHA models, respectively. These values are comparable to the MAE of 0.060 Å obtained for the static lattice constants. Similar to the static case, addition of some exact-exchange mixing further lowers the errors, with B86bPBE-25X-XDM giving MAEs of 0.033 Å and 0.053 Å, again bracketing the value of 0.039 Å obtained for the static lattice constants. Table II confirms that the Debye model is an excellent approximation for these compounds. The Debye approximation actually outperforms the more complex full QHA method, possibly due to error cancellation and a lower sensitivity to unphysical effects at high temperature, as seen in the case of lithium halides. Notably, the MAE between the calculated Debye and QHA cell parameters is only 0.022 Å, which is remarkable given the fact that the Debye model requires only the $E(V)$ curve as an input. The good performance of the Debye model for alkali halides has been noted before in the literature.[87]

D. Bulk moduli

Finally, we consider the performance of the XDM dispersion correction for the prediction of bulk moduli. Given the good performance of the Debye model for ionic solids, and the unphysical results of the full QHA in some cases, we consider vibrational effects calculated with the Debye model only in the following discussion.

There are two different kinds of experimental bulk moduli: isothermal [B_T, Eq. (8)], measured using static methods (e.g., x-ray

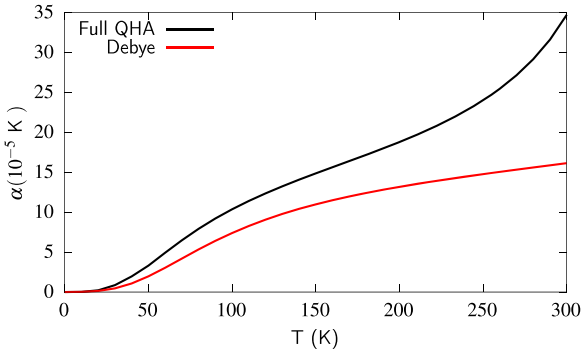

FIG. 3. Thermal expansivity (α) as a function of temperature in LiCl, predicted by B86bPBE-XDM with the full QHA (black) and Debye (red) models.

diffraction), and adiabatic [B_S, Eq. (9)], measured using dynamic methods (e.g., from ultrasonic elastic constants). They are related by Eq. (9) and, in the particular case of the alkali halides, can differ by several GPa. For instance, using B86bPBE-XDM and the Debye model, B_T = 66.9 GPa and B_S = 71.8 GPa for LiF. Since this difference is comparable to the errors from different density-functional approximations, clearly one must make sure to compare to the correct bulk modulus. This distinction is often disregarded in the literature.

Similar to the lattice constants, in order to compare calculated and experimental bulk moduli, one must account for vibrational effects. In the literature, vibrational corrections are typically limited to zero-point effects[93] (i.e., without the thermal contribution) or simply neglected.[3–5] The neglect of vibrational zero-point and thermal effects is sometimes appropriate, as in the calculation of relative stabilities discussed in Sec. III A and as noted by Nepal *et al.*[5] for cesium halides. However, doing the same for the bulk moduli is incorrect in general because the bulk modulus decreases significantly with temperature.

The temperature dependence of the bulk modulus can be quantified using experimental data for the temperature-derivative of the bulk modulus logarithm ($d \ln B/dT$) for various solids. For instance, Park and Sivertsen measured an adiabatic bulk modulus of 71.6 GPa at room temperature and ~75.5 GPa in the zero-temperature limit for BaO.[104] A simple fit to the linear, high-temperature portion of the experimental $B_S(T)$ curve yields $d \ln B/dT = -2.5 \times 10^{-4}$ K^{-1}, which results in a more than 4 GPa difference between the 0 K and room-temperature B_S values for BaO. This difference increases even further once vibrational zero-point effects are considered. For the alkali halides, $d \ln B/dT$ ranges from -2×10^{-4} to -10×10^{-4} K^{-1}, depending on the solid.[105] Therefore, there will be a very significant systematic error if static and experimental adiabatic bulk moduli are compared directly. This reasoning can be extended to other simple solids, making most density-functional benchmarks based on bulk moduli presented in the literature flawed.[3–5,93] More recent benchmark studies on bulk moduli do include both thermal and zero-point corrections,[106,107] but a consistent way of experimentally back-correcting room-temperature adiabatic and isothermal bulk moduli is still required.

Given that systematic bias has been introduced in previous density-functional benchmarks for bulk moduli, one must question

TABLE III. Adiabatic bulk moduli at room temperature, in GPa, computed with the PBE, B86bPBE, and B86bPBE-25X functionals, compared to experimental data. Three sets of data are shown: the static bulk moduli without dispersion corrections, the static bulk moduli with XDM, and the adiabatic bulk moduli calculated using the Debye model and with the XDM dispersion correction. ME: mean error and MAE: mean absolute error.

	Static B_0 (no dispersion)			Static B_0 (XDM)			B_S (XDM)			B_S
Name	PBE	B86bPBE	B86bPBE-25X	PBE	B86bPBE	B86bPBE-25X	PBE	B86bPBE	B86bPBE-25X	Expt.
LiF	66.92	65.89	73.10	87.69	80.00	86.60	78.36	71.77	77.02	69.6[105]
LiCl	31.72	31.03	32.71	39.86	37.27	38.78	36.11	32.41	33.84	31.7[105]
LiBr	25.67	25.04	26.12	33.79	30.18	31.00	30.83	26.70	27.46	25.6[105]
LiI	19.78	19.22	19.89	28.78	24.29	24.41	25.93	21.83	21.90	19.2[105]
NaF	44.79	43.93	48.45	58.01	58.83	64.56	52.09	52.22	57.42	48.5[105]
NaCl	23.65	23.03	24.17	35.00	34.19	34.12	31.32	30.44	30.40	25.1[105]
NaBr	19.37	18.82	19.54	29.36	28.59	28.37	25.71	25.08	24.94	20.6[105]
NaI	15.14	14.68	15.08	23.46	22.75	22.45	20.27	19.47	19.52	15.9[105]
KF	28.92	28.36	30.79	54.18	41.91	43.86	50.58	37.62	39.91	31.6[105]
KCl	16.24	15.82	16.47	37.65	26.30	25.64	34.13	23.86	23.06	18.2[105]
KBr	13.45	14.89	15.59	32.32	22.95	22.13	29.07	20.58	19.88	15.4[105]
KI	11.40	11.60	12.35	25.38	19.20	18.60	22.46	16.64	16.32	12.2[105]
RbF	24.52	24.01	25.98	54.61	38.01	38.79	51.34	35.55	35.74	27.7[105]
RbCl	14.17	13.80	14.34	37.34	25.58	24.91	33.82	22.93	21.47	16.2[105]
RbBr	12.08	12.29	13.06	31.48	22.23	21.53	28.31	19.60	18.17	13.8[105]
RbI	10.68	10.88	11.74	24.15	18.18	17.61	21.43	15.89	15.28	11.1[105]
CsF	20.46	20.01	21.57	56.97	35.98	36.06	54.13	32.65	32.44	23.9[105]
CsCl	16.06	16.52	13.03	36.38	25.67	26.11	34.25	23.10	23.25	18.3[105]
CsBr	13.51	13.92	12.02	32.63	22.14	22.26	30.80	20.00	17.73	15.9[105]
CsI	11.31	11.68	10.81	29.44	18.98	19.15	27.66	17.48	12.06	12.9[105]
MgO	149.00	147.91	165.70	155.54	155.45	173.56	147.24	147.18	164.96	163.9[108]
CaO	105.92	105.18	114.25	117.32	114.24	123.22	111.22	107.77	116.85	112.0[109]
SrO	84.53	83.84	91.44	98.32	91.86	99.75	95.87	89.01	95.76	91.0[110]
BaO	68.23	67.56	73.46	90.30	76.86	81.82	87.49	73.63	78.53	71.6[104]
ME	−2.68	−3.00	−0.42	14.09	6.66	8.89	10.36	2.98	4.67	
MAE	2.74	3.00	1.52	14.78	7.36	8.89	11.81	4.89	4.74	

how the conclusions were affected by this bias. It has been noted that application of dispersion corrections decreases agreement with experimental bulk moduli. For instance, Tao *et al.* avoided using PBE-vdW bulk moduli since they "slightly worsen the PBE bulk modulus."[3] Likewise, Klimeš *et al.*[4] observed that the MAEs of non-local functionals are generally worse than those obtained using much simpler GGA functionals. This is at odds with the observations for the lattice constants.

Table III provides a clue to resolve this contradiction. This table shows the static bulk moduli and room-temperature adiabatic bulk moduli, calculated with three different functionals, with and without dispersion, and compared to reference room-temperature B_S values. The experimental adiabatic bulk moduli reported were obtained from various sources in the literature,[104,105,108–110] and they are equal to the reference data used by Tao *et al.* in the case of alkali halides.[3]

Consistent with the observations of Tao *et al.*[3] and others, the agreement between static bulk moduli using uncorrected GGA functionals and the experimental bulk moduli is excellent. However, by our previous argument, this comparison is not appropriate because of the quite substantial vibrational contributions to the bulk moduli, which is evidenced in the difference between the static and B_S results in this table. The static bulk moduli calculated with dispersion-corrected functionals are substantially higher, resulting in a much worse agreement with experimental B_S data. However, the inclusion of vibrational effects brings the adiabatic bulk moduli back into reasonable agreement with experiment, at least in the cases of B86bPBE-XDM and B86bPBE-25X-XDM. Therefore, the apparent good performance of GGA functionals can be attributed to an (easily preventable) systematic bias introduced by the neglect of vibrational effects, which at room temperature have about the same magnitude as the dispersion contributions to the bulk moduli.

Importantly, Table III shows that PBE, which performs very well if the erroneous comparison between static and experimental bulk moduli is made, is the worst-performing functional once dispersion interactions and vibrational effects are taken into account. As in the case of lattice constants, we attribute the poorer performance of PBE-XDM to the underestimation of non-bonded repulsion due to the exchange enhancement factor, resulting in a gross overestimation of the bulk modulus. In sharp contrast, if functionals with a more appropriate exchange enhancement factor are used, such as B86bPBE-XDM or its 25% hybrid, then the error decreases to the 4–5 GPa range, with a slight systematic overestimation remaining, which could be attributed to our treatment of anharmonicity.

IV. DISCUSSION

B86bPBE-XDM has essentially the same cost as a semilocal functional calculation, and the dispersion correction has the simplicity of an asymptotic pairwise formula. The good performance of B86bPBE-XDM and its 25% hybrid functional (B86bPBE-25X-XDM) for ionic solids, together with their ability to treat molecular crystals,[52–56,111,112] layered materials,[62] surface adsorption,[57–59] and gas-phase molecules,[16,50,113,114] confirms that these methods are excellent candidates for the universal modeling of chemical processes in materials science. This adds further support to what we have stated in the past:[62] that asymptotic pairwise methods can be as accurate as their more complicated relatives if they correctly capture electronic many-body effects.

To support this point, it is interesting to compare the performance of B86bPBE-XDM with other functionals that are not based on an asymptotic dispersion energy expression. Given the abundance of results for non-local and other dispersion methods in the literature, we focus on a very recent paper by Kim *et al.*,[47] where the uMBD method, a modification of MBD,[15] is benchmarked for metallic, ionic, and van der Waals interactions. The authors stated that "uMBD conserves a better uniform accuracy over other methods across a wide range of systems,"[47] so we may take it as a representative sample of a modern non-asymptotic dispersion method.

While a full comparison is not possible because of the limited uMBD data presented,[47] uMBD underperforms in comparison to B86bPBE-XDM for common benchmark sets. For the S22 set of molecular binding energies,[115,116] uMBD has an MAE of 0.54 kcal/mol compared to 0.37 kcal/mol for B86bPBE-XDM. Similarly, for the X23 set of molecular lattice energies,[61,117] B86bPBE-XDM achieves an MAE of 0.85 kcal/mol,[16,78] while uMBD has an MAE of 1.2 kcal/mol. In addition, B86bPBE-XDM has been extensively applied to molecular crystal polymorphism,[53–56,111,112] demonstrating excellent performance for the prediction of experimental polymorph landscapes.

Moving to inorganic solids, the MAE in the alkali-halide lattice constants is 0.060 Å for B86bPBE-XDM, as shown above, while it is 0.047 Å for uMBD.[47] For surface adsorption, the sets reported for uMBD[47] and B86bPBE-XDM[57] are not equivalent, so we examine the individual systems for which adsorption energies have been calculated using both methods. For benzene on Au(111), the adsorption energies are 14.8 (B86bPBE-XDM) and 12.0 kcal/mol (uMBD), compared to the reference value of 16.7 kcal/mol. Similarly, for benzene on Ag(111), the adsorption energies are 15.7 (B86bPBE-XDM) and 11.5 kcal/mol (uMBD), compared to the reference value of 14.6 kcal/mol. A more meaningful comparison could be obtained with more data but, in these particular cases, the performance of B86bPBE-XDM far exceeds uMBD, which appears to systematically underestimate the adsorption energies. Finally, B86bPBE-XDM shows excellent performance for the calculation of interlayer separations (MAE = 0.072 Å) and exfoliation energies (MAE = 4.0 meV/Å^2) of layered materials, comparable to MBD-FI. The latter is similar to uMBD; unfortunately, Kim *et al.*[47] did not provide enough data about layered systems for a meaningful comparison.

Our analysis confirms the good performance and universality of B86bPBE-XDM for metallic, ionic, and molecular systems. When it comes to dispersion corrections, a principle of parsimony must apply. Asymptotic pairwise dispersion corrections are simple, cheap, and if they capture electronic many-body effects correctly,[68] they are comparable in quality if not better than the most complicated dispersion-corrected functionals.

V. CONCLUSIONS

In this article, we have studied the performance of several XDM-corrected functionals in the description of the relative

stability, lattice constants, and bulk moduli of simple ionic solids. XDM-corrected functionals have shown excellent performance in the description of non-covalent interactions in the past, and the purpose of this work is to establish that these functionals can also be used in the modeling of hard solids, such as ionic compounds.

The studied systems were simple ionic solids, including 20 alkali halides and 4 alkaline-earth oxides (MgO, CaO, SrO, and BaO). Three different aspects were considered: the relative stabilities of cesium-halide phases, the calculation of lattice constants and of bulk moduli. The prediction of polymorphism in the cesium halides is relatively simple, and we show that XDM and other dispersion-corrected functionals correctly identify the experimental phase of CsF (B1, rocksalt) and of CsCl, CsBr, and CsI (B2, CsCl). The use of a dispersion correction is essential in order to obtain the proper energy ranking, while vibrational effects have only a very minor role.

The lattice constant benchmark was carried out in two steps. First, we used the experimental data proposed by Tao *et al.*[3] that were back-corrected to remove vibrational effects and allow a direct comparison with the calculated static lattice constants. We find that B86bPBE-XDM and its 25% hybrid (B86bPBE-25X-XDM) perform excellently, with average errors of only 0.060 Å and 0.039 Å, respectively. The inclusion of dispersion corrections again decreases the error in the calculated lattice constants and, importantly, PBE-XDM has a considerably higher error (0.143 Å), which we attribute to the underestimation of non-bonded repulsion. We have noted previously that the effect of the exchange enhancement factor on non-bonded repulsion can be magnified for ionic interactions.[90] The improved performance of the hybrid functional is attributed to decreased delocalization error, which may be important in these systems. In the second step, we considered the calculated lattice constants at room temperature using the Debye and full QHA thermal models. The good performance of B86bPBE-XDM and B86bPBE-25X-XDM for the lattice constants is preserved, and we also note the excellent predictions achieved with the relatively crude Debye model.

Finally, we also considered the calculation of bulk moduli in ionic systems. It has been claimed in the literature that simple GGAs, such as PBE or PBEsol, are able to accurately predict experimental bulk moduli. We show that this is the result of a quite significant and uncontrolled error cancellation between missing dispersion and missing vibrational effects, which arises from comparing static (or zero-point corrected) bulk moduli and experimental bulk moduli. If the comparison is made including vibrational effects, then including dispersion is essential. As seen for the lattice constants, dispersion-corrected PBE is the worst-performing functional, which confirms that properly accounting for non-bonded repulsion through the exchange enhancement factor is necessary for ionic solids. Previous claims regarding the accuracy of simple semilocal functionals for the prediction of bulk moduli are marred by a preventable systematic bias in comparison with experimental data.

ACKNOWLEDGMENTS

This research was funded by the Natural Sciences and Engineering Research Council of Canada (NSERC; Grant No. RGPIN-05795-2016) and the Spanish Government (Grant Nos. RyC-2016-20301, PGC2018-097520-A-100, and RED2018-102612-T). The authors are grateful to Compute Canada and the MALTA Consolider supercomputing centre for computational resources. We thank an anonymous reviewer for pointing out to us the article where the uMBD method is presented.

DATA AVAILABILITY

The data that support the findings of this study are available from the corresponding author upon reasonable request.

REFERENCES

[1] G. A. DiLabio and A. Otero-de-la-Roza, Rev. Comput. Chem. **29**, 1 (2016).
[2] *Non-Covalent Interactions in Quantum Chemistry and Physics*, edited by A. Otero-de-la-Roza and G. DiLabio (Elsevier, 2017).
[3] J. Tao, F. Zheng, J. Gebhardt, J. P. Perdew, and A. M. Rappe, Phys. Rev. Mater. **1**, 020802(R) (2017).
[4] J. Klimeš, D. R. Bowler, and A. Michaelides, Phys. Rev. B **83**, 195131 (2011).
[5] N. K. Nepal, A. Ruzsinszky, and J. E. Bates, Phys. Rev. B **97**, 115140 (2018).
[6] F. Zhang, J. D. Gale, B. P. Uberuaga, C. R. Stanek, and N. A. Marks, Phys. Rev. B **88**, 054112 (2013).
[7] S. Grimme, A. Hansen, J. G. Brandenburg, and C. Bannwarth, Chem. Rev. **116**, 5105 (2016).
[8] J. Hermann, R. A. DiStasio, Jr., and A. Tkatchenko, Chem. Rev. **117**, 4714 (2017).
[9] S. Grimme, J. Comput. Chem. **27**, 1787 (2006).
[10] S. Grimme, J. Antony, S. Ehrlich, and H. Krieg, J. Chem. Phys. **132**, 154104 (2010).
[11] S. Grimme, S. Ehrlich, and L. Goerigk, J. Comput. Chem. **32**, 1456 (2011).
[12] E. Caldeweyher, S. Ehlert, A. Hansen, H. Neugebauer, S. Spicher, C. Bannwarth, and S. Grimme, J. Chem. Phys. **150**, 154122 (2019).
[13] E. Caldeweyher, J.-M. Mewes, S. Ehlert, and S. Grimme, Phys. Chem. Chem. Phys. **22**, 8499 (2020).
[14] A. Tkatchenko and M. Scheffler, Phys. Rev. Lett. **102**, 073005 (2009).
[15] A. Tkatchenko, R. A. DiStasio, R. Car, and M. Scheffler, Phys. Rev. Lett. **108**, 236402 (2012).
[16] E. R. Johnson, in *Non-Covalent Interactions in Quantum Chemistry and Physics*, edited by A. Otero-de-la-Roza and G. A. DiLabio (Elsevier, 2017), Chap. 5, pp. 169–194.
[17] S. N. Steinmann, G. Csonka, and C. Corminboeuf, J. Chem. Theory Comput. **5**, 2950 (2009).
[18] S. N. Steinmann and C. Corminboeuf, J. Chem. Theory Comput. **6**, 1990 (2010).
[19] S. N. Steinmann and C. Corminboeuf, J. Chem. Phys. **134**, 044117 (2011).
[20] S. N. Steinmann and C. Corminboeuf, J. Chem. Theory Comput. **7**, 3567 (2011).
[21] M. Dion, H. Rydberg, E. Schröder, D. Langreth, and B. Lundqvist, Phys. Rev. Lett. **92**, 246401 (2004).
[22] M. Dion, H. Rydberg, E. Schröder, D. C. Langreth, and B. I. Lundqvist, Phys. Rev. Lett. **95**, 109902 (2005).
[23] T. Thonhauser, V. Cooper, S. Li, A. Puzder, P. Hyldgaard, and D. Langreth, Phys. Rev. B **76**, 125112 (2007).
[24] O. A. Vydrov and T. Van Voorhis, Phys. Rev. Lett. **103**, 063004 (2009).
[25] O. A. Vydrov and T. Van Voorhis, J. Chem. Phys. **133**, 244103 (2010).
[26] O. A. Vydrov and T. Van Voorhis, J. Chem. Theory Comput. **8**, 1929 (2012).
[27] D. C. Langreth, B. I. Lundqvist, S. D. Chakarova-Käck, V. R. Cooper, M. Dion, P. Hyldgaard, A. Kelkkanen, J. Kleis, L. Kong, S. Li, P. G. Moses, E. Murray, A. Puzder, H. Rydberg, E. Schröder, and T. Thonhauser, J. Phys.: Condens. Matter **21**, 084203 (2009).
[28] G. A. DiLabio, Chem. Phys. Lett. **455**, 348 (2008).
[29] I. D. Mackie and G. A. DiLabio, J. Phys. Chem. A **112**, 10968 (2008).

[30]E. Torres and G. A. DiLabio, J. Phys. Chem. Lett. **3**, 1738 (2012).
[31]G. A. DiLabio, M. Koleini, and E. Torres, Theor. Chem. Acc. **132**, 1 (2013).
[32]O. A. von Lilienfeld, I. Tavernelli, U. Rothlisberger, and D. Sebastiani, Phys. Rev. Lett. **93**, 153004 (2004).
[33]I.-C. Lin, M. D. Coutinho-Neto, C. Felsenheimer, O. A. von Lilienfeld, I. Tavernelli, and U. Rothlisberger, Phys. Rev. B **75**, 205131 (2007).
[34]Y. Zhao, N. E. Schultz, and D. G. Truhlar, J. Chem. Phys. **123**, 161103 (2005).
[35]Y. Zhao and D. G. Truhlar, J. Chem. Phys. **125**, 194101 (2006).
[36]Y. Zhao and D. G. Truhlar, Theor. Chem. Acc. **120**, 215 (2008).
[37]R. Peverati, Y. Zhao, and D. G. Truhlar, J. Phys. Chem. Lett. **2**, 1991 (2011).
[38]R. Peverati and D. G. Truhlar, J. Chem. Theory Comput. **8**, 2310 (2012).
[39]T. Sato and H. Nakai, J. Chem. Phys. **131**, 224104 (2009).
[40]T. Sato and H. Nakai, J. Chem. Phys. **133**, 194101 (2010).
[41]J. Tao, J. P. Perdew, and A. Ruzsinszky, Phys. Rev. B **81**, 233102 (2010).
[42]J. Tao, J. P. Perdew, and A. Ruzsinszky, Proc. Natl. Acad. Sci. U. S. A. **109**, 18 (2012).
[43]J. Tao, J. P. Perdew, and A. Ruzsinszky, Int. J. Mod. Phys. B **27**, 1330011 (2013).
[44]A. Heßelmann, in *Non-Covalent Interactions in Quantum Chemistry and Physics*, edited by A. Otero-de-la-Roza and G. A. DiLabio (Elsevier, 2017), Chap. 3, pp. 65–136.
[45]A. D. Becke and E. R. Johnson, J. Chem. Phys. **127**, 154108 (2007).
[46]T. Gould, S. Lebègue, J. G. Ángyán, and T. Bučko, J. Chem. Theory Comput. **12**, 5920 (2016).
[47]M. Kim, W. J. Kim, T. Gould, E. K. Lee, S. Lebègue, and H. Kim, J. Am. Chem. Soc. **142**, 2346 (2020).
[48]A. Dalgarno and W. D. Davison, Adv. At. Mol. Phys. **2**, 1 (1966).
[49]A. Stone, *The Theory of Intermolecular Forces*, International Series of Monographs on Chemistry (Clarendon Press, 1997).
[50]A. Otero-de-la-Roza and E. R. Johnson, J. Chem. Phys. **138**, 204109 (2013).
[51]A. Otero-de-la-Roza and E. R. Johnson, J. Chem. Theory Comput. **11**, 4033 (2015).
[52]A. Otero-de-la-Roza and E. R. Johnson, J. Chem. Phys. **137**, 054103 (2012).
[53]A. Otero-de-la-Roza, B. H. Cao, I. K. Price, J. E. Hein, and E. R. Johnson, Angew. Chem., Int. Ed. **53**, 7879 (2014).
[54]S. R. Whittleton, A. Otero-de-la-Roza, and E. R. Johnson, J. Chem. Theory Comput. **13**, 441 (2017).
[55]S. R. Whittleton, A. Otero-de-la-Roza, and E. R. Johnson, J. Chem. Theory Comput. **13**, 5332 (2017).
[56]L. M. LeBlanc and E. R. Johnson, CrystEngComm **21**, 5995 (2019).
[57]M. S. Christian, A. Otero-de-la-Roza, and E. R. Johnson, J. Chem. Theory Comput. **12**, 3305 (2016).
[58]M. S. Christian, A. Otero-de-la-Roza, and E. R. Johnson, Carbon **118**, 184 (2017).
[59]M. S. Christian, A. Otero-de-la-Roza, and E. R. Johnson, Carbon **124**, 531 (2017).
[60]E. R. Johnson and A. Otero-de-la-Roza, J. Chem. Theory Comput. **8**, 5124 (2012).
[61]A. Otero-de-la-Roza and E. R. Johnson, J. Chem. Phys. **136**, 174109 (2012).
[62]A. Otero-de-la-Roza, L. M. LeBlanc, and E. R. Johnson, J. Phys. Chem. Lett. **11**, 2298 (2020).
[63]S. A. Tawfik, T. Gould, C. Stampfl, and M. J. Ford, Phys. Rev. Mater. **2**, 034005 (2018).
[64]A. Otero-de-la Roza and V. Luaña, Phys. Rev. B **84**, 184103 (2011).
[65]A. Otero-de-la Roza and V. Luaña, Phys. Rev. B **84**, 024109 (2011).
[66]E. R. Johnson and A. D. Becke, J. Chem. Phys. **124**, 174104 (2006).
[67]A. Otero-de-la-Roza and E. R. Johnson, J. Chem. Phys. **138**, 054103 (2013).
[68]A. Otero-de-la Roza, L. M. LeBlanc, and E. R. Johnson, Phys. Chem. Chem. Phys. **22**, 8266 (2020).
[69]A. D. Becke and E. R. Johnson, J. Chem. Phys. **124**, 014104 (2006).
[70]J. P. Perdew, K. Burke, and M. Ernzerhof, Phys. Rev. Lett. **77**, 3865 (1996).
[71]A. D. Becke, J. Chem. Phys. **85**, 7184 (1986).
[72]D. J. Lacks and R. G. Gordon, Phys. Rev. A **47**, 4681 (1993).
[73]Y. Zhang, W. Pan, and W. Yang, J. Chem. Phys. **107**, 7921 (1997).
[74]F. O. Kannemann and A. D. Becke, J. Chem. Theory Comput. **5**, 719 (2009).
[75]M. J. Gillan, J. Chem. Phys. **141**, 224106 (2014).
[76]A. D. Becke, J. Chem. Phys. **98**, 1372 (1993).
[77]C. Adamo and V. Barone, J. Chem. Phys. **110**, 6158 (1999).
[78]A. Otero-de-la-Roza, L. M. LeBlanc, and E. R. Johnson, J. Chem. Theory Comput. **15**, 4933 (2019).
[79]P. Giannozzi, O. Andreussi, T. Brumme, O. Bunau, M. Buongiorno Nardelli, R. Car, C. Cavazzoni, D. Ceresoli, M. Cococcioni, N. Colonna, I. Carnimeo, A. Dal Corso, S. de Gironcoli, P. Delugas, R. A. DiStasio, Jr., A. Ferretti, A. Floris, G. Fratesi, G. Fugallo, R. Gebauer, U. Gerstmann, F. Giustino, T. Gorni, J. Jia, M. Kawamura, H.-Y. Ko, A. Kokalj, E. Küçükbenli, M. Lazzeri, M. Marsili, N. Marzari, F. Mauri, N. L. Nguyen, H.-V. Nguyen, A. Otero-de-la-Roza, L. Paulatto, S. Poncé, D. Rocca, R. Sabatini, B. Santra, M. Schlipf, A. P. Seitsonen, A. Smogunov, I. Timrov, T. Thonhauser, P. Umari, N. Vast, X. Wu, and S. Baroni, J. Phys.: Condens. Matter **29**, 465901 (2017).
[80]P. E. Blöchl, Phys. Rev. B **50**, 17953 (1994).
[81]S. Baroni, S. de Gironcoli, A. Dal Corso, and P. Giannozzi, Rev. Mod. Phys. **73**, 515 (2001).
[82]A. Otero-de-la-Roza and V. Luaña, Comput. Phys. Commun. **182**, 1708 (2011).
[83]A. Otero-de-la-Roza, D. Abbasi-Pérez, and V. Luaña, Comput. Phys. Comm. **182**, 2232 (2011).
[84]P. Debye, Ann. Phys. **344**, 789 (1912).
[85]N. W. Ashcroft and N. D. Mermin, *Solid State Physics* (Thomson Learning, Inc., 1976).
[86]M. A. Blanco, E. Francisco, and V. Luaña, Comput. Phys. Commun. **158**, 57 (2004).
[87]M. Flórez, J. M. Recio, E. Francisco, M. A. Blanco, and A. M. Pendaás, Phys. Rev. B **66**, 144112 (2002).
[88]R. Sabatini, T. Gorni, and S. de Gironcoli, Phys. Rev. B **87**, 041108 (2013).
[89]J. Sun, A. Ruzsinszky, and J. P. Perdew, Phys. Rev. Lett. **115**, 036402 (2015).
[90]A. O. de la Roza and E. R. Johnson, J. Phys. Chem. A **124**, 353 (2020).
[91]J. Perdew, A. Ruzsinszky, G. Csonka, O. Vydrov, G. Scuseria, L. Constantin, X. Zhou, and K. Burke, Phys. Rev. Lett. **100**, 136406 (2008).
[92]P. Haas, F. Tran, and P. Blaha, Phys. Rev. B **79**, 085104 (2009).
[93]G. I. Csonka, J. P. Perdew, A. Ruzsinszky, P. H. T. Philipsen, S. Lebègue, J. Paier, O. A. Vydrov, and J. G. Ángyán, Phys. Rev. B **79**, 155107 (2009).
[94]E. R. Johnson, J. Chem. Phys. **135**, 234109 (2011).
[95]T. Bučko, S. Leb'egue, J. Hafner, and J. G. Ángyán, J. Chem. Theory Comput. **9**, 4293 (2013).
[96]J. Park, B. D. Yu, and S. Hong, Curr. Appl. Phys. **15**, 885 (2015).
[97]A. J. Cohen, P. Mori-Sánchez, and W. Yang, Science **321**, 792 (2008).
[98]A. D. Becke, J. Chem. Phys. **140**, 18A301 (2014).
[99]M.-C. Kim, E. Sim, and K. Burke, Phys. Rev. Lett. **111**, 073003 (2013).
[100]M.-C. Kim, H. Park, S. Son, E. Sim, and K. Burke, J. Phys. Chem. Lett. **6**, 3802 (2015).
[101]R. M. Wentzcovitch, B. B. Karki, M. Cococcioni, and S. de Gironcoli, Phys. Rev. Lett. **92**, 018501 (2004).
[102]R. Wyckoff, *Crystal Structures* (Interscience Publishers, New York, 1963).
[103]S. Grazulis, D. Chateigner, R. T. Downs, A. F. T. Yokochi, M. Quirós, L. Lutterotti, E. Manakova, J. Butkus, P. Moeck, and A. Le Bail, J. Appl. Cryst. **42**, 726 (2009).
[104]K.-O. Park and J. M. Sivertsen, J. Am. Ceram. Soc. **60**, 537 (1977).
[105]D. B. Sirdeshmukh, L. Sirdeshmukh, and K. G. Subhadra, *Alkali Halides: A Handbook of Physical Properties* (Springer-Verlag, 2001).
[106]F. Tran, J. Stelzl, and P. Blaha, J. Chem. Phys. **144**, 204120 (2016).
[107]G.-X. Zhang, A. M. Reilly, A. Tkatchenko, and M. Scheffler, New J. Phys. **20**, 063020 (2018).
[108]D. G. Isaak, O. L. Anderson, and T. Goto, Phys. Chem. Miner. **16**, 704 (1989).

[109]H. Oda, O. L. Anderson, D. G. Isaak, and I. Suzuki, Phys. Chem. Miner. **19**, 96 (1992).
[110]L.-G. Liu and W. A. Bassett, J. Geophys. Res. **78**, 8470, https://doi.org/10.1029/jb078i035p08470 (1973).
[111]Y. Yang, B. Rice, X. Shi, J. R. Brandt, R. Correa da Costa, G. J. Hedley, D.-M. Smilgies, J. M. Frost, I. D. W. Samuel, A. Otero-de-la-Roza *et al.*, ACS Nano **11**, 8329 (2017).
[112]B. Rice, L. M. LeBlanc, A. Otero-de-la-Roza, M. J. Fuchter, E. R. Johnson, J. Nelson, and K. E. Jelfs, Nanoscale **10**, 1865 (2018).
[113]G. A. DiLabio, E. R. Johnson, and A. Otero-de-la-Roza, Phys. Chem. Chem. Phys. **15**, 12821 (2013).
[114]A. Otero-de-la-Roza, E. R. Johnson, and G. A. DiLabio, J. Chem. Theory Comput. **10**, 5436 (2014).
[115]P. Jurečka, J. Šponer, J. Černỳ, and P. Hobza, Phys. Chem. Chem. Phys. **8**, 1985 (2006).
[116]M. S. Marshall, L. A. Burns, and C. D. Sherrill, J. Chem. Phys. **135**, 194102 (2011).
[117]A. M. Reilly and A. Tkatchenko, J. Chem. Phys. **139**, 024705 (2013).